AD-A038 464 ROME AIR DEVELOPMENT CENTER GRIFFISS AFB N Y F/G 20/5
LASER CHARACTERISTICS OF OPTICALLY PUMPED GAS PHASE MOLECULAR B--ETC(U)
JAN 77 F J WODARCZYK, H R SCHLOSSBERG

UNCLASSIFIED RADC-TR-77-50 NL

| OF |
AD
A038464

END

DATE
FILMED
5-77

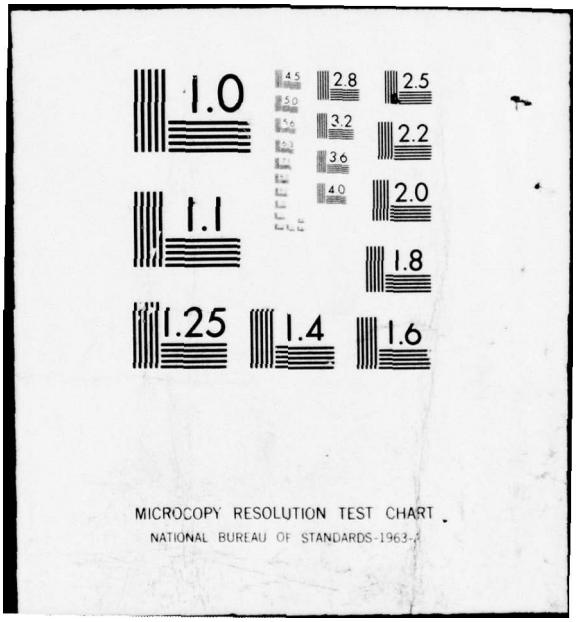
1.0
1.1
1.25
1.4
1.6
1.8
2.0
2.2
2.5
2.8
3.2
3.6
4.0
4.5
5.0
MICROCOPY RESOLUTION TEST CHART
NATIONAL BUREAU OF STANDARDS-1963-A

RADC-TR-77-50
IN-HOUSE REPORT
JANUARY 1977

Laser Characteristics of Optically Pumped Gas Phase Molecular Bromine

FRANCIS J. WODARCZYK
HOWARD R. SCHLOSSBERG

ROME AIR DEVELOPMENT CENTER
AIR FORCE SYSTEMS COMMAND
GRIFFISS AIR FORCE BASE, NEW YORK 13441

This report has been reviewed by the RADC Information Office (OI) and is releasable to the National Technical Information Service (NTIS). At NTIS it will be releasable to the general public, including foreign nations.

This technical report has been reviewed and approved for publication.

APPROVED:

ANDREW C. YANG
Acting Chief, Laser Technology Branch
Solid State Sciences Division

APPROVED:

ROBERT M. BARRETT, Director
Solid State Sciences Division

FOR THE COMMANDER:

Unclassified

SECURITY CLASSIFICATION OF THIS PAGE (When Data Entered)

REPORT DOCUMENTATION PAGE		READ INSTRUCTIONS BEFORE COMPLETING FORM
1. REPORT NUMBER RADC TR-77-50	2. GOVT ACCESSION NO.	3. RECIPIENT'S CATALOG NUMBER
4. TITLE (and Subtitle) LASER CHARACTERISTICS OF OPTICALLY PUMPED GAS PHASE MOLECULAR BROMINE		5. TYPE OF REPORT & PERIOD COVERED In-House
		6. PERFORMING ORG. REPORT NUMBER
7. AUTHOR(s) Francis J. Wodarczyk Howard R. Schlossberg		8. CONTRACT OR GRANT NUMBER(s)
9. PERFORMING ORGANIZATION NAME AND ADDRESS Deputy for Electronic Technology (RADC/ETSL) Hanscom AFB, MA 01731		10. PROGRAM ELEMENT, PROJECT, TASK AREA & WORK UNIT NUMBERS 61102F 23011101
11. CONTROLLING OFFICE NAME AND ADDRESS Deputy for Electronic Technology (RADC/ETSL), Hanscom AFB, MA 01731		12. REPORT DATE January 1977 13. NUMBER OF PAGES 26
14. MONITORING AGENCY NAME & ADDRESS (if different from Controlling Office)		15. SECURITY CLASS. (of this report) Unclassified 15a. DECLASSIFICATION/DOWNGRADING SCHEDULE

16. DISTRIBUTION STATEMENT (of this Report)

Approved for public release; distribution unlimited.

17. DISTRIBUTION STATEMENT (of the abstract entered in Block 20, if different from Report)

18. SUPPLEMENTARY NOTES

309 050

19. KEY WORDS (Continue on reverse side if necessary and identify by block number)

Optically pumped laser
Pulsed laser
Tunable laser
Visible laser
Infrared laser
Electronic transitions
Molecular bromine

20. ABSTRACT (Continue on reverse side if necessary and identify by block number)

Molecular bromine has been observed to lase when optically pumped on individual vibration-rotation lines. With no dispersive elements in the cavity, the output consists of several doublets, corresponding to P- and R-branch transitions from the excited state populated by the pump pulse to various vibrational levels of the ground state. The insertion of an intracavity prism causes a single doublet to lase, with a corresponding reduction in output power. In the current experiments the output wavelength was tunable from

over

DD FORM 1 JAN 73 1473 EDITION OF 1 NOV 65 IS OBSOLETE

Unclassified

SECURITY CLASSIFICATION OF THIS PAGE (When Data Entered)

6pgs

20. Abstract (Continued)

550 nm in the green to 750 nm in the near infrared for each transition pumped near 532 nm. The broadband efficiency was a few tenths of a percent, with the single-line output efficiency one tenth of that. A gain of 0.04 – 0.16 per cm at 6.8 torr and 300 K was estimated. This system offers a quasi-continuous tunable source of radiation ranging from the visible to the near infrared.

Preface

We would like to thank Dr. Audun Hordvik for helpful discussions and experimental assistance during many phases of this work. FJW also thanks Dr. Helge Kildal for clarification of the work on the I_2 laser system. We are indebted to Prof. Robert Field and Mr. Brooke Koffend of MIT for calculating Franck-Condon factors for higher vibrational levels of the Br_2 B-state.

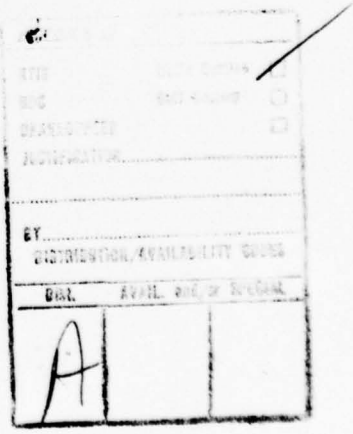

Contents

1. INTRODUCTION 7

2. EXPERIMENTAL 8

3. RESULTS 10

- 3.1 Pump Transitions 10
- 3.2 Lasing Process 13
- 3.3 Tunability of Laser Output 15
- 3.4 *Output Power* 16
  - 3.4.1 Power vs Br_2 Pressure 17
  - 3.4.2 Input vs Output Power 18
  - 3.4.3 Efficiency 19
- 3.5 Absorption Coefficients for Pumped Lines 19
- 3.6 Estimate of Gain 21
- 3.7 Miscellaneous Experiments 22

4. DISCUSSION 23

REFERENCES 25

Illustrations

1. Schematic Diagram of Experimental Arrangement 9

2. Total Br_2 Fluorescence as the Nd:YAG Pump Laser Intracavity Etalon is Swept 11

3. Potential Energy Diagram of Excited (B) and Ground (X) States of Br_2 14

Illustrations

4. Plot of Franck-Condon Factor ($q_{v'v''}$) vs Lower State Vibrational Quantum Number for v'=25-27 of the (79-81) Isotope 15

5. Peak Output Power in the Broadband Configuration vs Pressure of Active Material 17

6. Broadband Output Power vs Input Pump Laser Energy per Pulse 18

Tables

1. Assignment of Transitions That Result in Lasing 11

2. Comparison of Observed and Calculated Wavelengths (nm, in air) of Selected Lasing Transitions in Adjacent Pumped Transitions 12

3. Calculated Output Wavelength Range ($\lambda < 1000$ nm) of Lasing Transitions in Br_2 Pumped on (v'-v'') = (25, 26, 27-0) Transitions at 531.9 - 532.0 nm 16

Laser Characteristics of Optically Pumped Gas Phase Molecular Bromine

1. INTRODUCTION

Optical pumping of gas phase atoms and molecules has resulted in laser output from stimulated emission of rotational,[1] vibrational,[2] and electronic[3-10] transitions at wavelengths from the visible through the far infrared. The lasing species in these experiments have been pumped by various optical sources. Laser output on individual lines in the range 544 nm to 1.3 μm was obtained from I_2,[3]

(Received for publication 1 Feb 1977)

1. Chang, T. Y., and Bridges, T. J. (1970) Opt. Commun. 1:423.
2. Schlossberg, H. R., and Fetterman, H. R. (1975) Appl. Phys. Lett. 26:316.
3. Byer, R. L., Herbst., R. L., Kildal, H., and Levenson, M. D. (1972) Appl. Phys. Lett. 20:463.
4. Henesian, M., Herbst., R. L., and Byer, R. L. (1976) J. Appl. Phys. 47:1515.
5. Itoh, H., Uchiki, H., and Matsuoka, M. (1976) Opt. Commun. 18:271.
6. Leone, S. R., and Kosnik, K. G. (1977) A tunable visible and ultraviolet laser on S_2 ($B^3\Sigma_u^- - X^3\Sigma_g^-$), Appl. Phys. Lett., to be published.
7. Sorokin, P. P., and Lankard, J. P. (1971) J. Chem. Phys. 54:2184.
8. Djeu, N., and Burnham, R. (1974) Appl. Phys. Lett. 25:350.
9. Artusy, M., Holmes, N., and Siegman, A. E. (1976) Appl. Phys. Lett. 28:133.
10. Lin, M. C. (1974) IEEE J. Quantum Electron, QE-10:516.

stimulated emission from 526 to 850 nm was observed in Na_2,[4,5] and laser lines from 365 to 570 nm were found in S_2[6] when these molecules were pumped at various pulsed laser wavelengths. Two-photon pumping of molecular Cs_2, Rb_2, or K_2 using giant pulse laser beams resulted in stimulated emission from the Cs, Rb, or K atoms at wavelengths from 1.4 to 3.6 μm.[7] Continuous-wave laser emission in Hg at 546 nm has been observed in systems pumped by Hg lamps,[8,9] and lasing at 1.1, 1.2, and 2.6 μm has been measured in nitric oxide flash-photolyzed in the vacuum ultraviolet.[10]

We report here the observation of lasing in the visible and near infrared in gaseous room temperature Br_2, pumped at 532 nm with a frequency-doubled Q-switched Nd:YAG laser. In principle this system can result in discretely tunable output spanning from 0.5 to 3.5 μm, the widest output wavelength range of any optically pumped system reported so far.

2. EXPERIMENTAL

A schematic diagram of the experimental arrangement is shown in Figure 1. Room temperature Br_2 is contained in a static cell attached to a monel vacuum line. In early experiments the cell was a pyrex tube 11 cm long, 13 mm i.d., with quartz windows sealed on the Brewster angle ends. Later experiments used a stainless steel cell, 38 mm in diameter, having pyrex windows at each end mounted at Brewster's angle with 21 cm between window centers, and a quartz fluorescence window perpendicular to the optical axis at the midpoint of the cell. Br_2 pressures used ranged from 0.7 to 40 torr and were measured with an MKS Baratron corrosion-resistant capacitance manometer.

The cell and vacuum system were thoroughly seasoned with bromine before the experiments. The Br_2 used in the laser cavity was Mallinckrodt analytic reagent grade (> 99% pure). It was subjected to freeze-pump-thaw cycles, distilled, keeping only the middle portion of the distillate, and stored in a 1/2 liter pyrex bulb. Dupont Krytox fluorinated grease was used on the ground-glass surfaces. The bromine was subjected to a freeze-pump-thaw cycle before each new experiment as a precautionary measure.

The gaseous Br_2 was optically pumped on individual vibration-rotation lines using the frequency-doubled 532 nm output from a Chromatix model 1000E Q-switched Nd:YAG laser with an intracavity etalon (free spectral range 4.6 cm^{-1}) that narrowed the output to 0.03 cm^{-1}. The output energy of the pump laser was typically 0.6 mJ (0.8 mJ maximum) in a 200 ns pulse (60 ns FWHM) and was tunable over 0.1 nm by tilting the etalon. The beam waist at the output mirror is 0.52 nm, with a divergence half angle of 3.25×10^{-4} radian. It was found that

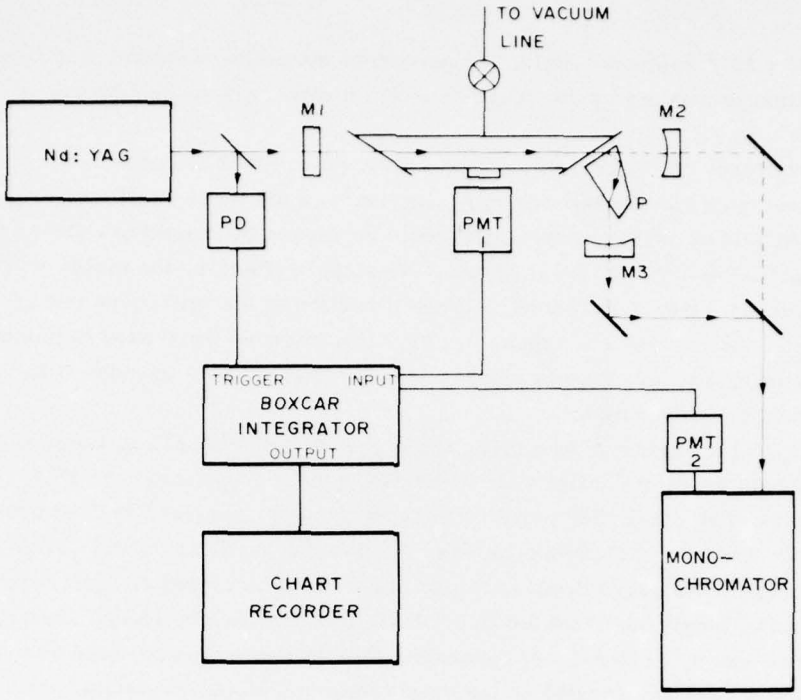

Figure 1. Schematic Diagram of Experimental Arrangement. Nd:YAG is the laser that produces narrow-band output 532 nm. M1, M2, and M3 are laser cavity mirrors, P is a Brewster-angle 90° prism, which can be inserted into the cavity when single line laser output is desired. PD is a photodiode that triggers the detection electronics. PMT1 and PMT2 are RCA 7326 photomultiplier tubes, and the monochromator is a half-meter Jarrell-Ash Ebert spectrometer

focusing the pump laser beam had little effect on the operation of the bromine laser, indicating that the optically pumped bromine was near saturation. Therefore, the unfocused pump beam was used in all experiments.

The laser cell was contained in an optical cavity 34 cm long with dielectric coated end mirrors. Two sets of mirrors were used, for lasing in the visible or in the red and near infrared. The input mirror was flat with the back side anti-reflection coated and the front surface > 90% transmitting at 532 nm and > 99% reflecting from 570 to 720 nm or from 640 to 1000 nm, depending on the lasing wavelengths being studied. The rear reflector was 1 m radius of curvature coated for 0.5% transmission from 550 to 680 nm or from 640 to 1000 nm. For this cavity the Br_2 laser beam waist at 580 (750) nm is calculated to be 0.30 (0.34) mm at the input mirror and 0.37 (0.42) mm at the output, with a far field diffraction angle

of 6.2 (7.1) x 10^{-4} radians. Thus, the portion of the active material that results in laser action is pumped by the central (most intense) part of the Chromatix laser beam.

The Br_2 laser cavity could be set up in two ways. With no intracavity element the cavity consisted of the cell and two mirrors, and the laser oscillated broadband. However, individual lasing wavelengths could be chosen by inserting a Brewster angle 90° prism into the cavity and tuning the output reflector, the single-wavelength output emerging perpendicular to the direction of the broadband lasing configuration, as indicated in Figure 1. Identical mirrors were used in mounts M2 and M3 so that it was easy to insert the prism and go from broadband to "single-line" laser operation.

The Br_2 laser emission was reflected into a Jarrell-Ash 1/2 m Ebert spectrometer (0.02 nm resolution) that was calibrated using a neon lamp. An RCA 7326 phototube was mounted on the output of the spectrometer and used to detect the laser lines. Another 7326 phototube was used to view the fluorescence from the Br_2 in the cell. The output from each phototube could be amplified (and, coincidentally, pulse lengthened) and fed into a PAR 160 Boxcar Integrator, the output of which was connected to a chart recorder. In this way a record could be made as the etalon (pump wavelength) or the spectrometer (output wavelength) was swept. The boxcar was triggered by a signal from a photodiode looking at reflected pump laser light.

An Eppley thermopile was used to determine the input laser energy, while the Br_2 laser power was measured using calibrated ITT biplanar photodiodes with S-1 surfaces. The photodiode outputs were observed on a dual beam oscilloscope, and measurements were made from photographic traces.

3. RESULTS

3.1 Pump Transitions

Since at room temperature approximately 79% of the Br_2 molecules of a given isotope are found in the $v''=0$ state and 17% in $v''=1$, the predominant absorptions at 532 nm are due to $B(^3\Pi^+_{ou}) \leftarrow X(^1\Sigma^+_{og})$ transitions $v' \geq 25 \leftarrow v''=0$ and $v' \geq 31 \leftarrow v''=1$. There is also some absorption from the $A(^3\Pi_{1u}) \leftarrow X(^1\Sigma^+_{og})$ continuum that is thought to peak near 530 nm.[11] Figure 2 shows the total emission from Br_2 emission as the pump wavelength is scanned over 0.1 nm. This spectrum is uncorrected for variations in the pump laser power as the etalon

11. Coxon, J.A. (1973) in Molecular Spectroscopy, ed. R.F. Barrow (Specialist Periodical Report), The Chemical Society, London, 1973, vol. 1, Ch. 4.

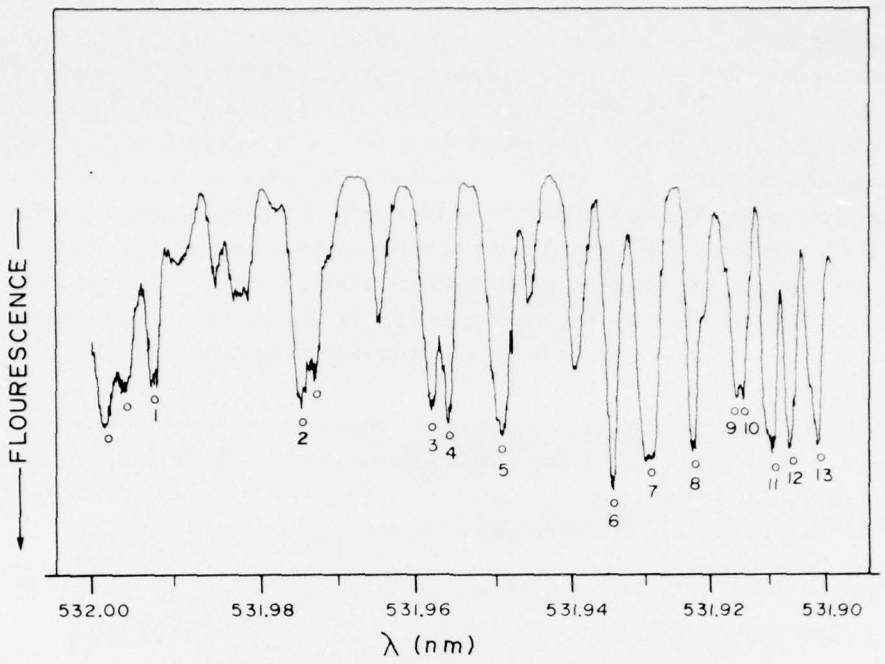

Figure 2. Total Br_2 Fluorescence as the Nd:YAG Pump Laser Intracavity Etalon is Swept. The spectrum is uncorrected for power and detector variations with wavelength. The circles denote lines that result in laser action when they are pumped. The numbered lines are listed and assigned in Table 1

Table 1. Assignment of Transitions That Result in Lasing

Line[a]	v'-v''	Rotational Transition	Isotope	λ_{calc}(nm in air)	$k_o/P(cm^{-1}torr^{-1})$
1	26-0	R(45)	79-79	531.994	0.0148
2	29-0	P(74)	79-81	531.976	0.0106
---	25-0	P(9)	79-81	531.971	0.0092
3	25-0	P(17)	79-79	531.954	0.0103
4	25-0	R(19)	79-79	531.952	0.0118
5	27-0	R(57)	79-81	531.948	0.0188
6	26-0	R(42)	79-81	531.933	0.0239
7	26-0	P(40)	79-81	531.927	0.0237
8	27-0	P(55)	79-81	531.923	0.0195
9	25-0	P(16)	79-79	531.912	0.0059
10	25-0	R(18)	79-79	531.911	0.0068
11	25-0	R(8)	79-81	531.908	0.0092
12	26-0	R(39)	81-81	531.903	0.0148
13	26-0	P(37)	81-81	531.901	0.0145
---	27-0	R(55)	81-81	531.891	0.0122

[a]Corresponds to numbering of lines in Figure 2.

is swept, and all the transitions are power broadened. Almost all of the absorption lines could be assigned to one of the above transitions of the three isotopes of Br_2. (Since ^{79}Br and ^{81}Br exist naturally in almost equal abundance, the Br_2 isotopes occur in the ratio (79-79):(79-81):(81-81) ≈ 1:2:1; absorptions due to all three isotopic combinations are readily observed.) The lines marked with a circle in Figure 2 are those that were observed to lase under the present pumping conditions. Table 1 lists the numbered lines and their spectroscopic assignments, which were based on the agreement between the measured lasing wavelengths and those calculated using the data of Barrow et al. [12] In all cases the lasing output consists of doublets corresponding to P- and R-branch transitions to $J''=J' \pm 1$ in the lower laser level.

Table 2 shows a comparison of some of the measured and calculated laser output wavelengths for adjacent pump transitions separated by 0.002 nm. It can be seen that the fit is good, and the assignments are unambiguous in each case. The larger wavelength discrepancies appear to be due to systematic errors in calibrating the spectrometer.

Table 2. Comparison of Observed and Calculated Wavelengths (nm, in air) of Selected Lasing Transitions in Adjacent Pumped Transitions

Pump transition: Line 13, 531.901 nm		Line 12, 531.903 nm	
λ_{obs}	$\Delta\lambda$(obs - calc)	λ_{obs}	$\Delta\lambda$(obs - calc)
550.20	0.04	550.53	0.02
a		580.48	0.02
		580.90	0.01
612.72	0.02		
613.18	0.06	613.16	0.04
		613.68	0.09
636.12	0.00		
636.56	-0.01	636.54	-0.02
		637.05	-0.01
674.08	0.04		
674.56	0.02	674.55	0.03
		675.06	-0.02
745.82	-0.02		
746.41	-0.04	746.38	-0.03
		747.04	-0.04

[a]Corresponding output not seen. See Section 3 of the text.

12. Barrow, R.F., Clark, T.C., Coxon, J.A., and Yee, K.K. (1974) J. Mol. Spectrosc. 51:428.

Table 2. Comparison of Observed and Calculated Wavelengths (nm, in air) of Selected Lasing Transitions in Adjacent Pumped Transitions (*Contd*)

Pump transition: Line 4, 531.952 nm		Line 3, 531.954 nm	
λ_{obs}	$\Delta\lambda$(obs - calc)	λ_{obs}	$\Delta\lambda$(obs - calc)
550.82	0.00	550.68	0.02
551.01	-0.02	550.84	0.01
581.26	0.03	581.05	-0.01
581.46	0.01	581.26	0.02
614.50	0.07	614.37	0.13
614.72	0.05	614.54	0.10
638.40	0.11	638.24	0.15
638.65	0.10	638.42	0.12
677.02	0.03		
677.31	0.05		

3.2 Lasing Process

Figure 3 shows potential energy curves for Br_2 and illustrates the processes by which Br_2 lases. The narrowed 532 nm radiation pumps molecules from the ($v''=0$, J'') level in the X state into a ($v'\geq 25$, $J'=J''\pm 1$) level in the excited B state. The excited molecules lase back down to one of the v'' levels shown. (Lasing can and almost certainly does occur to $v'' > 18$ levels, but the resulting radiation was outside the detection limits of the phototube used in these experiments. Hence, we are here restricting our discussion to lasing wavelengths less than 800 nm, implying $v'' \geq 18$.) Wavelengths corresponding to the solid lines in Figure 2 have been observed and match transitions with the larger Franck-Condon factors.[13] (See Figure 4.) The dotted line transition to $v'' = 1$ was not observed because of poor mirror reflectivity at 540 nm, but this transition is expected to lase with intensity comparable to the $v' = 2$ transition, which was the strongest lasing doublet observed. When operated in the broadband configuration, the relative intensities of the transitions are qualitatively given by the Franck-Condon factors $q_{v'v''}$. Therefore, the output power is concentrated more in the shorter wavelength output.

13. Appendix I to Ref. 12 and calculations performed by Prof. R.W. Field and Mr. B. Koffend of MIT.

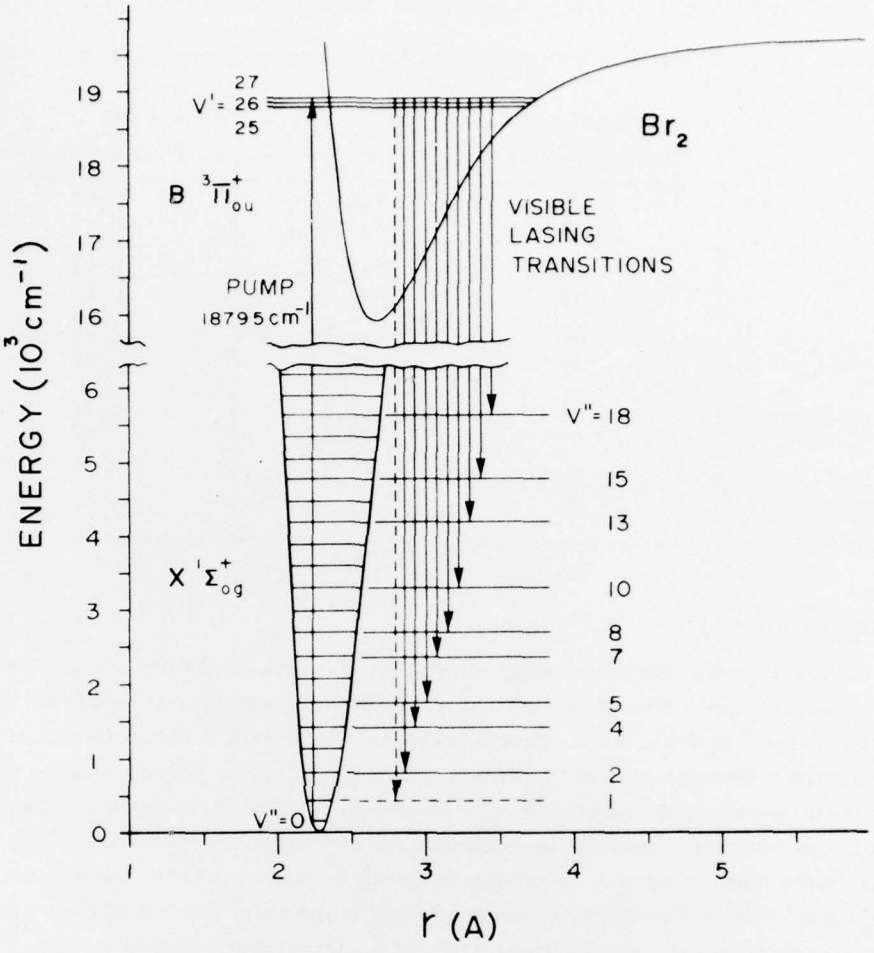

Figure 3. Potential Energy Diagram of Excited (B) and Ground (X) States of Br_2. The pump transition at 18795 cm^{-1} (532 nm in air) transfers population to one of the vibrational-rotational levels shown in the B-state, from which stimulated emission to any of the indicated ground state vibrational levels can occur

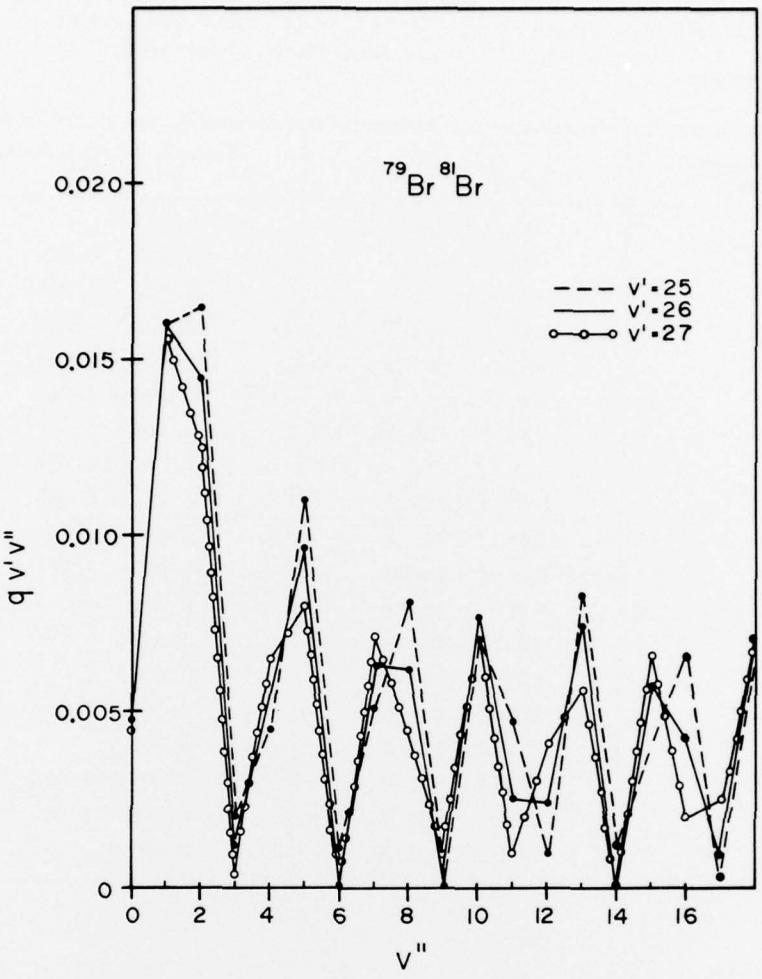

Figure 4. Plot of Franck-Condon Factor ($q_{v'v''}$) vs Lower State Vibrational Quantum Number for v'=25-27 of the (79-81) Isotope

3.3 Tunability of Laser Output

Table 3 lists the range of discrete output wavelengths < 800 nm that result when the pump wavelength is changed by 0.1 nm. It is seen that there is at least 10 times the wavelength range in output for a 0.1 nm sweep of the input pump wavelength. Furthermore, the tuning range widens as the output wavelength increases, so that by 750 nm a 0.1 nm sweep of the pump results in a 4.9 nm sweep of the output.

Table 3. Calculated Output Wavelength Range ($\lambda < 1000$ nm) of Lasing Transitions in Br_2 Pumped on (v''-v'') = (25, 26, 27-0) Transitions at 531.9-532.0 nm. Output for v''=1 to 18 has been observed in these experiments

Lower Laser v'' Level	λ_{air} range (nm)	Franck-Condon factor (v'=25-27)
1	540.7 - 541.7	0.016
2	550.2 - 551.3	0.013 - 0.017
4	569.8 - 571.3	0.004 - 0.007
5	580.1 - 581.7	0.008 - 0.011
7	601.5 - 603.5	0.005 - 0.007
8	612.7 - 614.9	0.004 - 0.008
10	636.1 - 638.7	0.007 - 0.008
13	674.0 - 677.4	0.007 - 0.008
15	701.4 - 705.3	0.006 - 0.007
16	718.0 - 719.9	0.006
18	745.8 - 750.7	0.006 - 0.007
20	779.1 - 781.2	0.006
21	795.0 - 801.1	0.008
23	830.5 - 837.8	0.007
24	853.9 - 857.2	0.006
25	870.8 - 873.2	0.005
26	889.1 - 897.7	0.007 - 0.008
28	931.8 - 941.7	0.006 - 0.007
29	961.1 - 965.6	0.008

3.4 Output Power

In the course of the experiments it was found that one of the pump lines (#13) that resulted in strong output power in the broadband configuration produced laser output that appeared red to the eye when the "visible mirrors" were used. In this cavity the broadband laser output from all the other pump lines appeared yellow. It is not known why the output from pumping this line (a 26-0, P(37), 81-81 line) is different from the output of its immediate neighbor (#12, 26-0, R(39), 81-81), which differs only by two rotational quanta. It is conceivable that an accidental coincidence between the yellow (26-5, 580 nm) laser transitions and Br_2 absorptions reduces the gain sufficiently to quench the lasing on those transitions. The red laser output was convenient because of both its intensity and its unique color. For example, when the pump laser wavelength drifted, it was easy to return to the

proper transition by tuning the etalon back to the red output. This broadband red output was used for studies of the output power vs both Br_2 pressure and input energy.

3.4.1 POWER VS Br_2 PRESSURE

Figure 5 shows a plot of the peak broadband output power (as measured with a calibrated photodiode) vs Br_2 pressure when line 13 is pumped with 0.6 mJ per pulse. The output pulse has a FWHM of 60 ns, and a total pulse length approximately 140 ns. Since the pump laser used hops from one transverse mode to another ($1/2L = 0.007\ cm^{-1}$, $\Delta\nu_L \simeq .03\ cm^{-1}$) with each shot, the wavelength does not always coincide with the peak of the Br_2 transition being pumped ($\Delta\nu_D \simeq 0.017\ cm^{-1}$). Consequently, the Br_2 laser output varies in power from shot to shot. The output power plotted corresponds to the peak output observed in a set of 50 pulses, since it was felt that this represents more truly the possible power output obtainable from a better frequency-stabilized pump source. The smoothness of the curve, indicating the reproducibility of the data, supports the

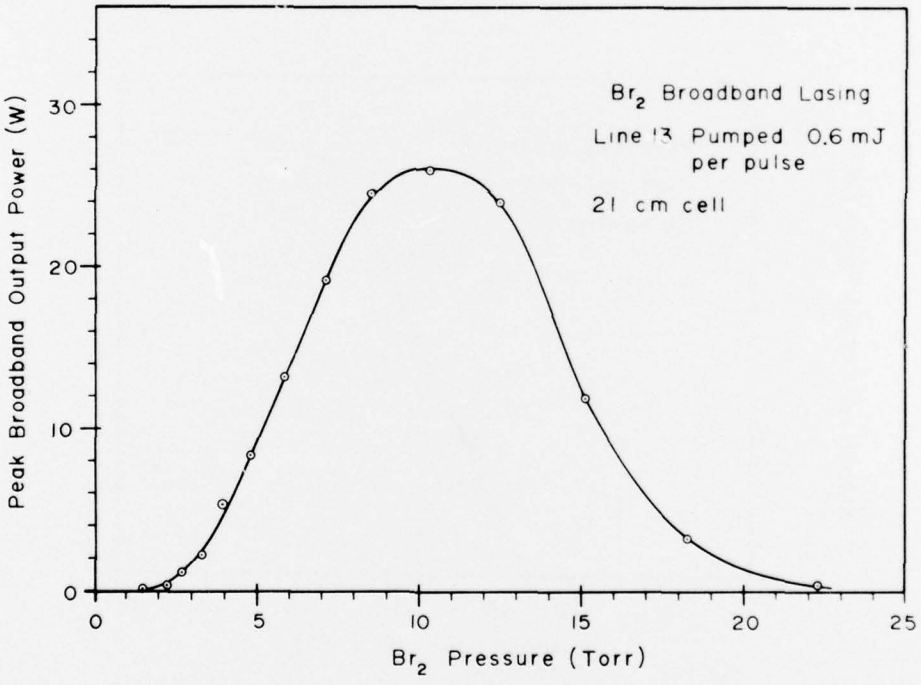

Figure 5. Peak Output Power in the Broadband Configuration vs Pressure of Active Material

reasonableness of this approach. Other methods of determining the power, such as signal averaging 200 pulses or taking the average of 50 shots on a photograph of oscilloscope traces, yield the same type of curve.

From Figure 5 it is seen that under the stated conditions (0.6 mJ pump energy on line 13, 21 cm path length) the output peaks near 10 torr. The pressure at which this peak occurs is expected to shift to higher values as the pump energy is increased, since the peak is determined by the point at which the change in the pump rate (a first order process) in the gain expression is less than the change in the rate of collisional quenching of the excited state (effectively a second-order process). That this is true is verified by experiment: when the input pump energy per pulse is changed to 0.4 mJ, the peak of the output power occurs around 7.5 torr, while at 0.46 mJ it lies between 8 and 9 torr.

3.4.2 INPUT VS OUTPUT POWER

Figure 6 shows how the broadband output power varies with input energy at constant pressure. At this pressure, threshold is near 0.25 mJ per pulse, and the pump transition appears to saturate at about 0.5 mJ/pulse. There are two other indications that we are approaching saturation at higher input powers:

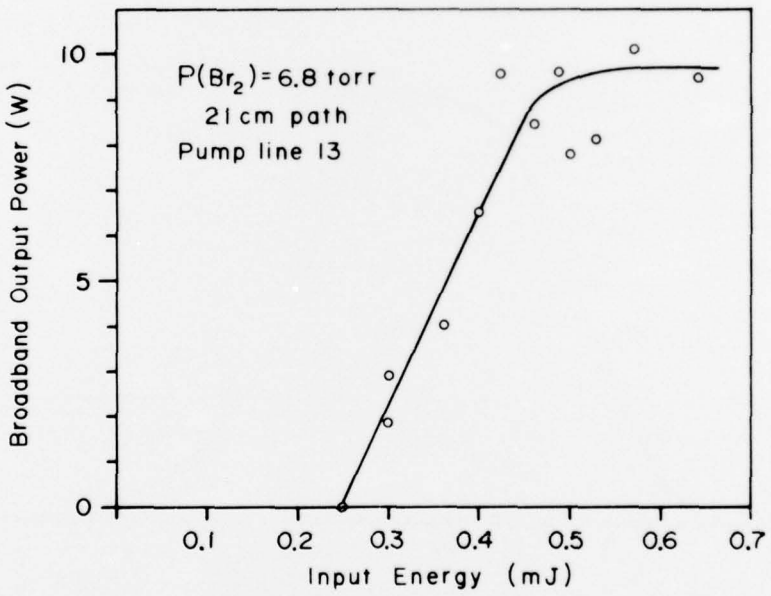

Figure 6. Broadband Output Power vs Input Pump Laser Energy per Pulse

(a) There is little discernible effect on the laser threshold and output power when the input bean is focused into the cell; and

(b) Absorbances $\left(\log \{ I_o/I \}\right)$ were several factors smaller if they were measured with the laser Q-switched instead of un-Q-switched.

3.4.3 EFFICIENCY

For an input power of about 10 kW we find, under optimum conditions, peak output powers on the order of tens of watts broadband and a few watts in the single-line lasing configuration. The efficiency of this Br_2 laser is thus on the order of a few tenths of a percent broadband, or hundredths of a percent single line.

3.5 Absorption Coefficients for Pumped Lines

Beer's law states that at low light intensities I_o incident on a gas of pressure P, the transmitted intensity I can be related to the path length ℓ by the equation

$$\log (I_o/I) = k\ell = \alpha P \ell \ . \tag{1}$$

At the peak of an absorption, $k(\nu=\nu_o) \equiv k_o = \alpha_m P$, and for a line of full width at half maximum of $\Delta\nu$,

$$\frac{k_o}{N_1} = \sigma_0 = \frac{2c^2 A_{21}\, g_2 \sqrt{\log 2/\pi}}{8\pi \nu^2\, g_1\, \Delta\nu} \ , \tag{2}$$

where N_1 is the density of molecules in the lower level of the absorbing transition $2 \leftarrow 1$, σ_0 is the peak absorption cross section per molecule for the transition, g_j is the degeneracy of the jth level, and A_{21} is the rate of spontaneous emission for the absorbing transition. For a Doppler-broadened (Gaussian) line

$$\Delta\nu_D = 2\frac{\nu}{c}\sqrt{\frac{2\ kT\ \log 2}{m}} \tag{3}$$

and, since

$$A_{21} = \frac{64\pi^4\ \nu^3}{3hc^3 g_2} S_J \mid R_e \mid^2 q_{v'v''} \ , \tag{4}$$

we get

$$\frac{k_o}{N_1} = \sigma_0 = \frac{8\pi^3}{3hg_1} S_J \mid R_e \mid^2 q_{v'v''} \sqrt{\frac{m}{2\pi kT}} \ , \tag{5}$$

where S_J is the rotational line strength for this transition and $|R_e|^2$ is the square of the electronic part of the transition moment, which is usually assumed to be constant. This equation is more useful if we express it in terms of quantities we measure in the laboratory. If we denote the isotopic fraction by i (0.50 for 79-81, 0.25 for 79-79 or 81-81) and the total partation function by Q, then from Boltzmann's equation

$$N_1 = \frac{ig_i' e^{-E_1/kT}}{Q} N \tag{6}$$

and the ideal gas law

$$P = NkT , \tag{7}$$

Eq. (5) can be rearranged to give

$$\frac{k_o}{P} = \frac{8\pi^3 i}{3hQ} \frac{g_1'}{g_1} \sqrt{\frac{mkT}{2\pi}} S_J |R_e|^2 e^{-E_1/kT} q_{v'v''} . \tag{8}$$

Here both g_1 and Q take account of nuclear spin statistics for homonuclear diatomics. Since ^{79}Br and ^{81}Br each have nuclear spin $I = \frac{3}{2}$, the statistical weight for even J rotational levels is $I(2I+1) = 6$ and for odd J it is $(I+1)(2I+1) = 10$. (The partition function for these homonuclear isotopes correspondingly includes a factor of $(2I+1)^2 = 16$ to account for the nuclear spin and a factor of 1/2 to account for the symmetry.) For the heteronuclear 79-81 isotopes, all rotational levels have the same weight, which cancels in the division of g_1/Q; thus the statistical weight for the herteronuclear diatomics need not be considered. Using the value of $|R_e|^2 = 0.12\ D^2$ measured in Ref. 14 together with Eq. (8), values of k_o/P in units of $cm^{-1}\ torr^{-1}$ at 300 K were calculated for all of the pumped transitions and are listed in Table 1. These numbers agree within 50% with the values measured using two planar photodiodes and a PAR model 162 dual channel boxcar integrator. However, because no precautions were taken to stabilize the laser wavelength and force it into single-mode operation, the calculated absorption coefficients are felt to be more accurate.

The measurement of the continuum A ←X absorption, however, is not expected to be subject to these constraints, and the value of $(2\pm1)\times10^{-3}\ cm^{-1}\ torr^{-1}$ is found for $k_{continuum}/P$ at 300 K. This number may be compared with $6.7\times10^{-3} cm^{-1} torr^{-1}$

14. Zaraga, F., Nogar, N.S., and Moore, C.B. (1976) Transition moment, radiative lifetime and quantum yield for dissociation of the $^3\Pi_{o^+u}$ state of $^{81}Br_2$, to be published.

measured at 558 nm[14] and the value of 6×10^{-4} cm^{-1} $torr^{-1}$ predicted[11] to be the peak absorption coefficient for A ← X near 530 nm. All these absorption measurement data imply that the A ← X continuum absorption is a smaller fraction of the total absorption (B ← X and A ← X) at 532 nm than the 89% inferred from photofragment spectroscopy experiments.[15] The fact that the linewidth of the frequency-doubled Nd:glass laser used in the photofragment work was not as narrow as those of the current experiments and of Zaraga et al[14] means that not all of the radiation could be efficiently absorbed by the sharp, widely spaced B ← X absorption lines. Hence, the absorption by the continuum may have been effectively enhanced. The interpolated value[16] of k_o/P at 532 nm and 298 K is 7×10^{-3} cm^{-1} $torr^{-1}$, measured with a broadband excitation source, which similarly samples relatively more continuum than discrete transitions.

3.6 Estimate of Gain

Let us consider a system in which molecules initially in state 1 are excited to state 2, from which they can radiate or lase down to a state 3. If the density of molecules in state 1 in thermal equilibrium is designated N_1^0, then when the transition 2 ← 1 is saturated,

$$g_2 N_1 = g_1 N_2 \tag{9}$$

and, assuming $N_1 + N_2 = N_1^0$, then

$$N_2 = \frac{g_2 N_1^0}{g_1 + g_2} \simeq 1/2 N_1^0 . \tag{10}$$

The gain per pass on the laser transition 2 → 3 is

$$g = \alpha_m \ell = \sigma_\ell N_2 \ell . \tag{11}$$

Here α_m is the peak value of the amplification curve, ℓ is the length of the active material, and σ_ℓ is the cross section per molecule for the laser transition. We can therefore estimate the gain for the Br_2 laser transitions in terms of the cross sections for the pump and laser transitions using Eqs. (5) and (11):

---

15. Oldman, R.J., Sander, R.K., and Wilson, K.R. (1975) J. Chem. Phys. 63:4252.

16. Passachier, A.A., Christian, J.D., and Gregory, N.W. (1967) J. Phys. Chem. 7:937.

$$\frac{\sigma_\ell}{\sigma_p} = \frac{(S_j q_{v'v''}/d_3)_\ell}{(S_j q_{v'v''}/d_1)_p} \quad . \tag{12}$$

Because the line strength is given by $S_J = J$ (P-branch) or J+1 (R-branch), $(S_J)_\ell = (S_J)_p \pm 1$, where the subscript refers to the laser or pump transition. Similarly, since $J_3 = J_1$ or $J_1 \pm 2$ (because only P- and R-branch pump and laser transitions are allowed), and because we are dealing here with mostly high J transitions (see Table 1), we make the approximations $(S_J)_\ell \simeq (S_J)_p$ and $g_1 \simeq g_2 \simeq g_3$. Eq. (12) therefore becomes

$$\sigma_\ell \sim \frac{(q_{v'v''})_\ell}{(q_{v'v''})_p} \sigma_p \quad . \tag{13}$$

Since $(k_o)_p = \sigma_p N_1^0$, by Eq. (10) we find that

$$(k_o)_\ell \simeq \frac{1}{2} \frac{(q_{v'v''})_\ell}{(q_{v'v''})_p} (k_o)_p \quad . \tag{14}$$

Because $(q_{v'v''})_\ell \sim 2\,(q_{v'v''})_p$ for the transitions that lase (see Figure 4), we get

$$g \sim (k_o)_p \ell \quad . \tag{15}$$

That is, the magnitude of the gain is given by that of the absorption coefficients for the pump transitions. At 6.8 torr pressure, for example, $g \sim 0.04\text{-}0.16$ cm^{-1} or 0.8 - 3.4 per pass for a 21 cm active length.

We can also estimate the gain using the method of Ref. 3. Using the reported lifetime and quenching cross section at 532 nm,[17] we calculate at 6.8 torr an excited state lifetime (t_2) of 11 ns. We estimate the loss per pass in the laser cavity to be 5% or less, and measure the time after pumping at which laser action begins (t_b) to be typically 75 ns. Using these values and the expression for gain found in Ref. 3, we find $g \sim 0.05 - 0.06$ cm^{-1} = 1.1 - 1.3 per pass in good agreement with the estimate made above. This can be compared with the gain of 0.024 cm^{-1} for room temperature I_2 found in Ref. 3.

3.7 Miscellaneous Experiments

An attempt was made to determine whether the upper state population can be rotationally relaxed rapidly enough by collisions with argon to enable quasi-tunable

17. Capelle, G., Sakurai, K., and Broida, H. P. (1971) J. Chem. Phys. 54:1728.

lasing, in analogy with dye lasers. However, the only effect of the argon at the available pump power was to quench the lasing at pressures $\gtrsim$ 65 torr.

An experiment was also tried in which the Nd:YAG pump laser was operated without the intracavity etalon. In this case, the spectral width of the pump pulse was 1 cm^{-1} (0.03 nm) and it overlapped several of the pump transitions. The Br_2 lased very weakly, but no studies were made of the spectral output wavelengths and power, so that it is not known how many transitions were made to lase.

4. DISCUSSION

From the preceding discussion it is clear that the molecular bromine laser is an attractive source of tunable radiation in certain regions of the visible and near infrared spectrum, out to about 3 μm. The exact output wavelengths depend on the transition pumped, and, as seen in Section 3.3, a small change in pump wavelength produces a large change in output wavelength, the range increasing with increasing wavelength of the lasing radiation. Due to the high density of vibration-rotation lines available, the output tunability is quasi-continuous. In the 532 nm pump region used in this study, we calculate on the average 12 absorption lines per cm^{-1} from all isotopic species originating from $v'' = 0$ and 1 levels, some regions having as many as 10 transitions in 0.1 cm^{-1}. The spectroscopic constants are known well enough so that they can be relied on to predict lasing wavelengths to within 0.1 nm up to fairly high v'' lower laser levels.

The Br_2 laser performance compares favorably with respect to that of the room temperature I_2 laser. The efficiency of the output is slightly less but of similar magnitude. However, the higher pressure attainable at room temperature with Br_2 (150 - 500 torr) means that higher gain is possible with this system than with room temperature I_2 in the same call length, provided adequate pump power is available to overcome collisional quenching losses[17] due to the higher pressures involved. Furthermore, the range of output laser lines extends farther into the infrared for the Br_2 laser.

The Br_2 laser can also be used for an accurate determination of spectroscopic information about high lying vibrational levels of the ground state and as a means of measuring Franck-Condon factors. Furthermore, in the single-line configuration one can selectively populate specific vibrational levels in the ground state with a large number of molecules. Such capability would be useful for experiments in state-selected chemistry, such as energy transfer, reaction kinetics, photochemistry, and isotope separation.

One might be tempted to envision a flashlamp-pumped Br_2 laser analogous to a dye laser system. Such a laser would be attractive because of its very wide

tuning range, low cost, and long life under flashlamp excitation. However, because of the large self-quenching cross sections for the B state[17] and collisional dissociation processes, the high pressures needed to broaden the spectrum and achieve the rotational relaxation necessary for continuous tunability would be counter-productive to lasing.

The ultimate power possible from the Br_2 laser is limited by the very fast radiationless processes (spontaneous pre-dissociation) postulated[17] and measured[18] for the B state levels, which lower the maximum attainable energy storage per unit volume. And although the gain could be augmented by increasing the path length of the active medium, other problems and complications (such as, physical size) associated with this solution must be dealt with.

Nonetheless, the optically pumped Br_2 laser is a convenient source of low power, discretely tunable radiation extending from the visible out to 3 μm in the infrared. It furthermore serves as a prototype system from which much can be learned about the nature of optically pumped gas phase diatomic molecule laser systems.

18. Lum, R. M., and McAfee, K. B., Jr. (1975) J. Chem. Phys. 63:5029.

References

1. Chang, T. Y., and Bridges, T. J. (1970) Opt. Commun. 1:423.
2. Schlossberg, H. R., and Fetterman, H. R. (1975) Appl. Phys. Lett. 26:316.
3. Byer, R. L., Herbst, R. L., Kildal, H., and Levenson, M. D. (1972) Appl. Phys. Lett. 20:463.
4. Henesian, M., Herbst, R. L., and Byer, R. L. (1976) J. Appl. Phys. 47:1515.
5. Itoh, H., Uchiki, H., and Matsuoka, M. (1976) Opt. Commun. 18:271.
6. Leone, S. R., and Kosnik, K. G. (1977) A tunable visible and ultraviolet laser on S_2 ($B^3\Sigma_u^- - X^3\Sigma_g^-$), Appl. Phys. Lett., to be published.
7. Sorokin, P. P., and Lankard, J. R. (1971) J. Chem. Phys. 54:2184.
8. Djeu, N., and Burnham, R. (1974) Appl. Phys. Lett. 25:350.
9. Artusy, M., Holmes, N., and Siegman, A. E. (1976) Appl. Phys. Lett. 28:133.
10. Lin, M. C. (1974) IEEE J. Quantum Electron, QE-10:516.
11. Coxon, J. A. (1973) in Molecular Spectroscopy, ed. R. F. Barrow (Specialist Periodical Report), The Chemical Society, London, 1973, vol. 1, Ch. 4.
12. Barrow, R. F., Clark, T. C., Coxon, J. A., and Yee, K. K. (1974) J. Mol. Spectrosc. 51:428.
13. Appendix I to Ref. 12 and calculations performed by Prof. R. W. Field and Mr. B. Koffend of MIT.
14. Zaraga, F., Nogar, N. S., and Moore, C. B. (1976) Transition moment, radiative lifetime and quantum yield for dissociation of the $^3\Pi_{o^+u}$ state of $^{81}Br_2$, to be published.
15. Oldman, R. J., Sander, R. K., and Wilson, K. R. (1975) J. Chem. Phys. 63:4252.
16. Passachier, A. A., Christian, J. D., and Gregory, N. W. (1967) J. Phys. Chem. 71:937.

17. Capelle, G., Sakurai, K., and Broida, H. P. (1971) J. Chem. Phys. 54:1728.
18. Lum, R. M., and McAfee, K. B., Jr. (1975) J. Chem. Phys. 63:5029.

MISSION
of
Rome Air Development Center

RADC plans and conducts research, exploratory and advanced development programs in command, control, and communications (C^3) activities, and in the C^3 areas of information sciences and intelligence. The principal technical mission areas are communications, electromagnetic guidance and control, surveillance of ground and aerospace objects, intelligence data collection and handling, information system technology, ionospheric propagation, solid state sciences, microwave physics and electronic reliability, maintainability and compatibility.

Printed by
United States Air Force
Hanscom AFB, Mass. 01731